Nanotoxicology

Direct and indirect CeO₂ nanoparticles toxicity for *Escherichia coli* and *Synechocystis*

Ophélie Zeyons [a]; Antoine Thill [a]; Franck Chauvat [b]; Nicolas Menguy [c]; Corinne Cassier-Chauvat [bd]; Cédric Oréar [b]; Jean Daraspe [e]; Mélanie Auffan [f]; Jérôme Rose [f];Olivier Spalla [a]

[a] CEA, IRAMIS, Laboratoire Interdisciplinaire sur l'Organisation Nanométrique et Supramoléculaire, Gif-surYvette, [b] CEA, iBiTec-S, SBIGeM, LBI, Bat 142, CEA SACLAY, F91191 Gif sur Yvette, [c] Institut de Minéralogie et Physique des Milieux Condensés UMR 7590, CNRS, Université Pierre et Marie Curie, Université Paris Diderot, Institut de Physique du Globe de Paris, Paris [d] CNRS, URA 2096, F-91191 Gif sur Yvette CEDEX, [e] CEA, iBiTec-S, Laboratoire du Trafic Membranaire, CEA SACLAY, F91191 Gif sur Yvette, [f] CEREGE, UMR 6635 CNRS/Aix Marseille Université, Europôle de l'Arbois, 13545 Aix en Provence, , France

PLEASE SCROLL DOWN FOR ARTICLE

informa
healthcare

Direct and indirect CeO$_2$ nanoparticles toxicity for *Escherichia coli* and *Synechocystis*

OPHÉLIE ZEYONS[1], ANTOINE THILL[1*], FRANCK CHAUVAT[3], NICOLAS MENGUY[2], CORINNE CASSIER-CHAUVAT[3,4], CÉDRIC ORÉAR[3], JEAN DARASPE[5], MÉLANIE AUFFAN[6], JÉRÔME ROSE[6], & OLIVIER SPALLA[1]

[1]*CEA, IRAMIS, Laboratoire Interdisciplinaire sur l'Organisation Nanométrique et Supramoléculaire, Gif-surYvette,* [2]*Institut de Minéralogie et Physique des Milieux Condensés UMR 7590, CNRS, Université Pierre et Marie Curie, Université Paris Diderot, Institut de Physique du Globe de Paris, Paris,* [3]*CEA, iBiTec-S, SBIGeM, LBI, Bat 142, CEA SACLAY, F91191 Gif sur Yvette,* [4]*CNRS, URA 2096, F-91191 Gif sur Yvette CEDEX,* [5]*CEA, iBiTec-S, Laboratoire du Trafic Membranaire, CEA SACLAY, F91191 Gif sur Yvette, and* [6]*CEREGE, UMR 6635 CNRS/Aix Marseille Université, Europôle de l'Arbois, 13545 Aix en Provence, France*

Abstract

Physico-chemical interactions between nanoparticles and cell membranes play a crucial role in determining the cytotoxicity of nanoparticles, which may thereby vary depending on the nature of the target microorganisms. We investigated the responses of two different models of unicellular bacteria to cerium oxide (CeO$_2$) nanoparticles. These organisms are: *Synechocystis* PCC6803 a representative of environmentally important cyanobacterial organisms (producer of biomass for aquatic food chains), and *Escherichia coli* a representative of intestine-colonizing bacteria. Coupling physico-chemical (adsorption isotherms and electrophoretic mobility), biological (survival tests), microscopical (SEM, TEM and EDS) and spectroscopic (XANES) methods, we enlightened two distinct mechanisms for the CeO$_2$ nanoparticles toxicological impact: A 'direct' mechanism that requires a close contact between nanoparticles and cell membranes, and an 'indirect' influence elicited by the acidity of nanoparticles stabilizing agents. We showed that *E. coli* is sensitive to the 'direct' effects of nanoparticles, whereas *Synechocystis* being protected by extracellular polymeric substances preventing direct cellular contacts is sensitive only to the 'indirect' mechanism. Consequently, our findings demonstrate the importance of the 'direct/indirect' effects of nanoparticles on cell fitness, a phenomenon that should be systematically investigated with appropriate techniques and dose metrics to make meaningful environmental and/or health recommendations.

Keywords: *Nanoparticles, toxicity, cerium oxide, Extracellular Polymeric Substances (EPS), microscopy, survival tests, adsorption isotherm, electrophoretic mobility*

Introduction

Nanoparticles have opened the routes for promising medical diagnostics and treatments (Moghimi et al. 2005; Minchin 2008), new devices in electronic (Ko et al. 2007) and improved properties for materials for which interfaces control the desired functions. In some cases, these prospects became a biotechnological reality as several nanoparticles related technologies have emerged as new products on the market. For example, CeO$_2$ nanoparticles are already used as diesel vehicle combustion catalysts (5–10 ppm in fuel tank). Consequently, exposure levels to CeO$_2$ nanoparticles have increased (Park et al. 2008), and

challenge human health through direct contacts, dissemination and accumulation into the environment.

The very small size of nanoparticles enables them to interact with biological systems at the sub-cellular scale (membranes, proteins, or DNA molecules), thereby challenging cell growth and survival. A strong societal demand has now emerged to *a priori* protect workers, consumers and the environment, and to develop a full corpus of basic knowledge and databases in the emerging field of *nanotoxicity* (Oberdörster et al. 2007). Therefore, several papers have recently studied the impact of nanoparticles on animals or mammalian cells (Derfus et al. 2004; Kirchner et al. 2005; Shukla et al. 2005; Franklin et al. 2007; Yacobi et al. 2007)

Correspondence: Antoine Thill, CEA Saclay, DSM/IRAMIS/SIS2M, Laboratoire Interdisciplinaire sur l'Organisation Nanométrique et Supramoléculaire, 91191 Gif-sur-Yvette, France. Email: antoine.thill@cea.fr

and bacteria (Brayner et al. 2006; Yoon et al. 2007; Lu et al. 2008; Neal 2008). However, they led to contrasted conclusions even when the studied biological targets were similar (Tarnuzzer et al. 2005; Auffan et al. 2006; Chen et al. 2006). This is unambiguously due to the lack of standardized tests crucial to the development of reproducible, i.e., robust conclusions that are required for meaningful risk predictions (Colvin 2003; Nel et al. 2006). In this objective, we presently report a detailed study of the nanoparticles/bacteria physico-chemical interactions and their relations with classical survival and membrane alteration tests. Therefore, we studied the effects of ceria (CeO$_2$) nanoparticles, a relevant model for environmental issues (Mai et al. 2005; Ozawa 2006; Park et al. 2008), on two evolutionary-distant microorganisms *Synechocystis* (photoautotrophic, spherical morphology) and *Escherichia coli* (heterotrophic, cylindrical shape). Our main purpose was to gain a fundamental understanding of the influence of well dispersed nanoparticles in interaction with relevant physiologically-different micro-organisms. Accordingly, a special care has been devoted to control the state of agglomeration of the nanoparticles by properly choosing the medium of dispersion. A second important issue of the study was the use of a range of concentrations covering different types of potential exposition: From a low range as expected for the life-cycle of manufactured nanoparticles in the environment to a high range as it may happen during an accidental release.

Materials and methods

Nanoparticles

All tests were performed starting from a CeO$_2$ nanoparticles dispersions of 10 g.kg^{-1} prepared the day before use by dispersion of a wet powder (Rhodia patent [Chane-Ching 1987]) composed of CeO$_2$ (HNO$_3$)$_{1/2}$,5H$_2$O in ultrapure water (UPW, 18.2 megaohm-cm). These nanoparticles have been thoroughly characterized (Spalla and Kékicheff 1997) as ellipsoidal monocrystallites of 7 nm in diameter, with a specific surface of 400 m^2.g^{-1} and a point of zero charge of 10.

The filtrate of nanoparticles was obtained by ultrafiltration of nanoparticles solution in an Amicon ultrafiltration cell unit equipped with a 10 kDa membrane (regenerated cellulose, Millipore).

Microbial strains and growth conditions

Synechocystis PCC6803 (hereafter *Synechocystis*), the widely-used cyanobacterium (Koksharova and Wolk 2002), was chosen as a representative model

of cyanobacteria, the most abundant photosynthetic organisms on Earth that make up a large part of the biomass for the food chain. *Synechocystis* was grown at 30°C under shaking (180 rpm) and continuous white light (2,500 lux) in MM (i.e., BG11 medium completed with Na$_2$CO$_3$ (3.8 mM) and buffered with Hepes, pH = 7.5). The cultures were kept exponentially growing through repeated sub-cultivations.

The RR1 strain of *E. coli*, the best-known model of heterotrophic bacteria (Neal 2008), was grown in Luria Bertani (LB) medium under shaking in the dark at 37°C. For every assay, a new culture was prepared from a frozen storage sample that was pre-cultivated the night before the assay.

Exposition of cells to nanoparticles

A special care was devoted to measure the state of dispersion of the nanoparticles in the medium of contact with the studied microorganisms. The stability of nanoparticles was checked with dynamic light-scattering experiments (DLS) performed on a zetasizer nanoZS (Malvern). The first two growth media studied, LB and MM for *E. coli* and *Synechocystis*, respectively, led to a massive aggregation due to their high ionic strength. Therefore, to reduce nanoparticles aggregation we also used salt-depleted contact media such as a synthetic moderately-hard water (SMHW) prepared from ultrapure water (UPW) as recommended by the US Environmental Protection Agency (NaHCO$_3$ 96 mg/l; CaSO$_4$, 2H$_2$O 60 mg/l; MgSO$_4$ 60 mg/L and KCl 4 mg/l).

Synechocystis and *E. coli* cultures were centrifuged at 20°C (for 10 min at 4500 *g* and 3 min at 4500 *g*, respectively) washed and resuspended three times in either UPW or SMHW. The concentrations of the resulting cell suspensions were adjusted by dilution in the appropriate UPW or SMHW water at the final optical density (OD) of 0.5 at 580 nm (~ 2.5 10^7 cells/ml for *Synechocystis*) or 2 at 600 nm (~ 6.8 10^8 cells/ml for *E. coli*) prior to exposure of 2 ml cell aliquotes with 100 µl aliquots of freshly prepared nanoparticles suspensions mixed by vortexing. The resulting cell suspensions contained a final concentration of CeO$_2$ nanoparticles ranging from 0 ppm (control sample) to 240 ppm, a wide range of concentrations going from potential environmental conditions (Park et al. 2008) to accidental acute exposures.

Survival tests measured through Colony Forming Units (CFU) assays

Cell suspensions with or without CeO$_2$ nanoparticles were incubated for 3 h in relevant incubators, serially

diluted in the test medium and plated onto the appropriate growth media (LB or MM) solidified with agar (1.5 and 1% w/v, respectively). The resulting colonies (CFU) were counted after one day (*E. coli*) or 10 days (*Synechocystis*) of growth and the survival rate was calculated as the ratio of the CFU number in the stressed versus unstressed (control) samples. The numbers reported are the mean value, and standard deviations, obtained after three independent repetitions of the assays.

Membrane integrity assays (Live/Dead tests)

Live/Dead® *BacLight*™ *Bacterial Viability* Kits (Molecular Probes) contain a mixture of both SYTO9 stain that labels all cells and propidium iodide that can only penetrate into cells with damaged membranes (dead cells). First, we verified the absence of direct interactions between the fluorescent dyes and the nanoparticles. As expected, the corresponding mixture emitted no fluorescence. Then, nanoparticles-treated samples (and untreated control cells) were mixed with an appropriate amount of *Live/Dead*® stain mixture in a black 96-microplate, which were shaken for 15 min under darkness. Fluorescence emitted at 530 nm and 630 nm, following excitation at 485 nm, was measured with a microplate reader SpectraMax M2-Molecular Devices. The percentage of living cells was calculated as the ratio of fluorescence emission (530/630) from stressed versus unstressed cells. The numbers reported are the mean value and the standard deviations obtained from three independent repetitions of the assays.

Adsorption isotherms and electrophoretic mobility

Cells suspensions were treated (or not, control samples) with the nanoparticles for 30 min prior to centrifugation (10 min at 4500 g) to yielding cell-less supernatants in which the CeO_2 content was assayed through electrophoresis analysis. For this purpose, the CeO_2 nanoparticles of the supernatants were first reduced and dissolved upon mixing with Mohr's salt ($FeSO_4$ (NH_4)$_2$ $SO_4.6H_2O$). The resulting samples were analyzed with a Beckman Coulter capillary electrophoresis, using a mix of HIBA (hydroxyisobutyric acid, Aldrich) and UVCAT1 (Waters) as electrolytes. Ce^{3+} concentrations were obtained as the measure of the area using a calibration established with the same protocol performed in absence of cells. The concentrations of adsorbed CeO_2 were deduced from the analyzed concentrations of Ce^{3+} and thus of free CeO_2 in the

supernatants. The isotherms were reported as the quantity (mg) of adsorbed CeO_2 per apparent outer surface of the bacteria. For suspensions with an OD of 0.5 for *Synechocystis* and 2 for *E. coli*, the specific surface value is 0.25 m^2/l for *Synechocystis* cells suspensions (approximating a *Synechocystis* cell to a 1 μm radius sphere) and 1.2 m^2/l for *E. coli* cells suspensions (rod of 1.5 μm in length flanked with two half spheres of 0.4 μm in diameter).

Electrophoretic mobility was measured with a zetasizer Nano ZS from Malvern. Disposable transparent electrophoretic mobility cells were used and the analytical calculations were carried out using the monomodal mode.

Electron microscopy experiments (TEM, STEM, EDS)

Samples for electron microscopy were prepared as those for the CFU survival tests. Following the 3 h nanoparticles treatment, samples were fixed with glutaraldehyde 2% for 1 h, washed with UPW water, permeabilized with metaperiodate 1% for 15 min, washed with UPW, and post-fixed with Karnovsky medium (1% osmium tetraoxide, 15 mg/ml potassium ferrocyanide) for 90 min. Samples were embedded in 2% agar, dehydrated in graded ethanol baths (70–100%), and embedded in Epon resin. Ultrathin sections (90 nm) were prepared with an ultramicrotome (UCT-FCS Leica Microsystems, Vienna, Austria) equipped with a diamond knife (Diatome AG, Biel, Switzerland). They were deposited on carbon-formvar nickel grid (Agar scientific) and stained with lead citrate (Reynold's lead) or uranyl acetate. Observations were carried out on a Philips CM12 electron microscope (FEI, Eindhoven, The Netherlands) operated at 80 kV, equipped with a US1000 Gatan camera.

Localization of nanoparticles was determined with a JEOL 2100F TEM/STEM operating at 200 kV. The High Angle Annular Dark Field (HAADF) imaging technique produces images with strong compositional information due to the Z-contrast. The regions with brighter contrast in STEM HAADF images indicate the presence of the heaviest element, i.e. regions with high concentrations of Ce atoms. The localization was confirmed through X-ray Energy Dispersive Spectroscopy (XEDS) elemental mapping using the Ce Lα line.

SEM samples prepared as CFU samples were fixed with a mixture of glutaraldehyde (2.5%) and alcian blue (0.15%) overnight, washed three times in UPW, deposited on aluminium pin stubs purchased from Agar Scientific, critical point-dried with CO_2, and observed with an Hitachi SEM.

XANES

XANES (X-ray Absorption Near Edge Structure) experiments were carried out on the FAME beam line (BM30b) at the European Synchrotron Radiation Facilities in Grenoble (France). The energy was set to Cerium L_3-edge. Solid samples were prepared as those used for CFU test, lyophilized, mixed with boron nitride and pellets shaped prior to the measurement. The samples were maintained at $-170°C$ with N_2 liquid to avoid beam damage. The data were obtained after performing standard procedure for pre-edge subtraction, normalization and fitted with linear combination of Ce^{III} and Ce^{IV} references compounds.

Results

The influence of nanoparticles on the survival of *Synechocystis* and *E. coli* was quantified using the Colony Forming Unit (CFU) assay and *Live/Dead* test (LD) (See Figure 1).

A 3 h exposure to CeO_2 nanoparticles in UPW induced different effects for *Synechocystis* and *E. coli*. A clear decrease of the cell viability was observed with *Synechocystis* exposed to low nanoparticles concentrations, followed by a plateau at 20–25% of survival for nanoparticles concentrations exceeding 60 ppm. Both the CFU and *Live/Dead* techniques gave the same values of cell survival to nanoparticles excepted for a concentration of 30 ppm yielding the most flocculated cell suspension. By contrast, these two techniques yielded different survival results for nanoparticles treated-*E. coli* cells. The standard CFU counting assay that really measures cell viability, i.e., the ability
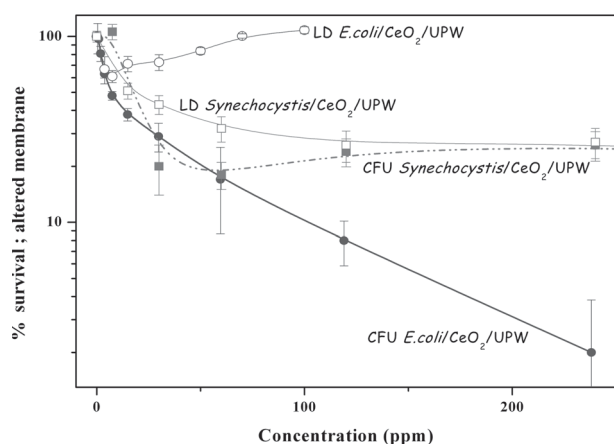
to divide thereby yielding colonies on solid growth medium, showed a dose-response effect. Indeed it steadily decreased down to 2% for 240 ppm of CeO_2, in agreement with previous observations (Thill et al. 2006). In contrast the *Live/Dead* test, which estimates cell survival based on the internalization of fluorescent dyes, suggested that only low doses of nanoparticles (around 10 ppm) were toxic (60% survival) and that this toxicity could be relieved with higher nanoparticles doses. This artefact will be addressed in the discussion.

Returning to *Synechocystis,* to check whether some components in the nanoparticles suspensions, other than the nanoparticles themselves, might participate to the nanoparticles-elicited toxicity (Pfaller et al. 2009), we used the *Live/Dead* assay to compare the survival of cells exposed to nanoparticles suspensions or only to their filtrate (Figure 2).

We found that the filtrates were as toxic as the full nanoparticles suspensions. This filtrate toxicity could arise from the presence of soluble Ce^{3+} ions and/or nitric acid molecules associated with the nanoparticles. To investigate these possible causes, we compared the survival rates of *Synechocystis* exposed to nanoparticles suspensions in ultra pure water (UPW) or in synthetic moderately hard water (SMHW), which contains ions that can counteract nitric acid. In strong contrast with UPW, no nanoparticles toxicity was observed in SMHW. This difference is directly linked to the pH of the *Synechocystis* cultures exposed to increasing amounts of nanoparticles suspensions in UPW and SMHW (Figure 2). In UPW, the additions of CeO_2 or nitric acid decreased the pH from 9–4.5, a very unfavorable value for the survival of cyanobacteria that prefer alkaline pH. By contrast, in

Figure 1. CFU of *Synechocystis* (■) and *E. coli* (•) after an exposition of 3 h to CeO_2 nanoparticles in UPW. *Live/Dead* assays of *Synechocystis* (□) and *E. coli* (○) exposed for 3 h to CeO_2 nanoparticles in UPW.
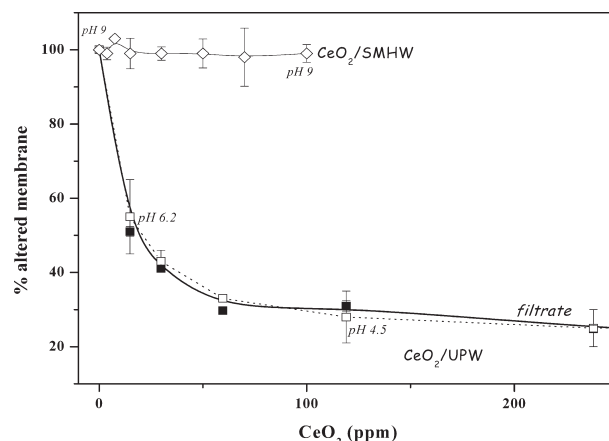
Figure 2. *Live/Dead* assays of membrane alteration for *Synechocystis* cells exposed for 3 h in UPW to CeO_2 nanoparticles suspension (■), to the filtrate of the same nanoparticles suspension (□) and to CeO_2 nanoparticles in SMHW (◇). The evolution of the pH of the suspension is reported close to the points.

SMHW, the buffering effect of $NaHCO_3$ did not allow the addition of nanoparticles to decrease the pH below 8. These data are consistent with the findings that toxicity experiments (CFU) performed in the standard 'MM' growth medium of *Synechocystis* that contains pH buffering HEPES and carbonate molecules showed no reduction of cell survival to nanoparticles exposure for 3 h or longer (24 h). As already mentioned, MM medium induces nanoparticles aggregation but these aggregates may have been toxic at least in the range of a one day exposure. This is again linked to the buffering effect of both the Hepes and carbonate ions contained in the MM. Collectively our findings support the major role of the pH of CeO_2 nanoparticles suspensions in their toxicity to *Synechocystis*.

For *E. coli* the comparison of toxicity between nanoparticles suspensions and their nanoparticles-free filtrates were measured by CFU tests only, to avoid the above-mentioned *Live/Dead* artifact (Figure 1). The results reported in the Figure 3 showed that nanoparticles suspensions decreased *E. coli* survival (10% for $[CeO_2] = 100$ ppm) more than their corresponding filtrate (70%). Hence, the mortality of *E. coli* exposed to CeO_2 nanoparticles is much more imputable to nanoparticles per se than to their environment

To understand the different sensitivities of the two types of bacteria, the physicochemical interactions between the cells and the CeO_2 nanoparticles were followed at different length scales. First, at the macroscopic scale, the stabilities of the two bacterial suspensions were altered by the addition of CeO_2 nanoparticles. *Synechocystis* cultures flocculated and settled quickly in response to 15 ppm CeO_2 (Figure 4A). For concentration larger than 30 ppm, the cultures flocculated but the aggregates remained
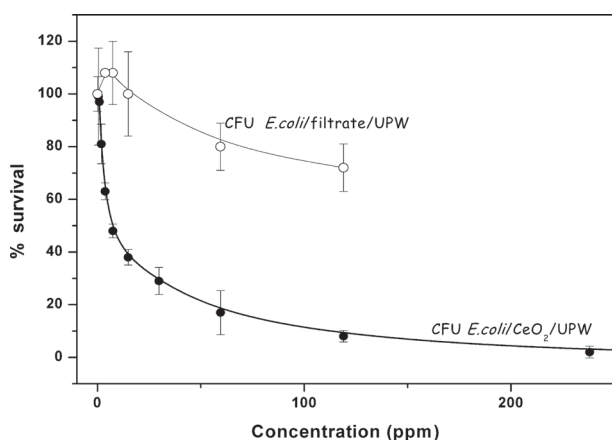
Figure 3. CFU of *E. coli* cells after an exposition of 3 h in UPW to CeO_2 nanoparticles suspension (•) and to the filtrate of the same nanoparticles suspension (○).
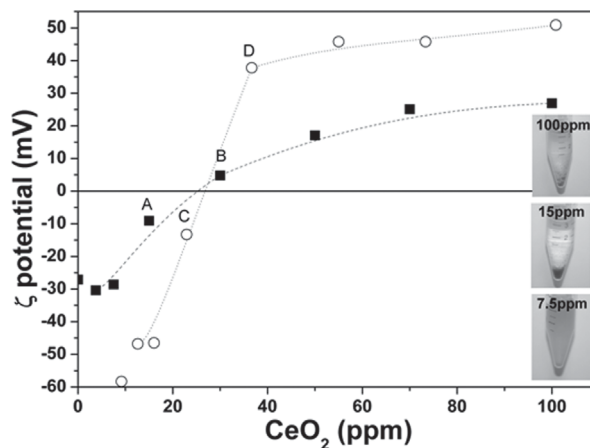
A
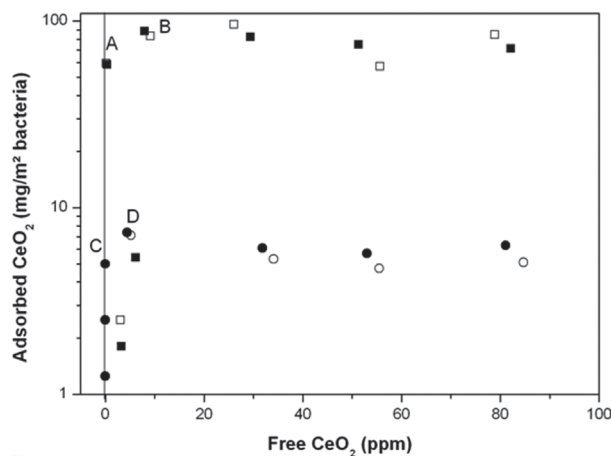
B

Figure 4. (A) Electrophoretic mobility of *Synechocystis* (■) and *E. coli* (○) versus CeO_2 concentrations in UPW. The images show different states of suspension of the *Synechocystis* cultures along the isotherm. (B) Adsorption isotherms of ceria nanoparticles: *Synechocystis* (■,□), *E. coli* (○,•).

in suspension. Cultures of *E. coli* behaved similarly though flocculation was obtained only for a narrow concentration range of nanoparticles around 15 ppm.

We studied the influence of increasing amounts of nanoparticles on the electrophoretic mobilities of cells in UPW (Figure 4A). The initial electrophoretic mobilities are -4.5 and -2 μm·cm/V·s for *E. coli* and *Synechocystis*, respectively. For *E. coli*, the electrophoretic mobility showed a sharp increase up to zero with nanoparticles addition (Figure 4A, between points C and point D) followed by a charge reversal. In the case of *Synechocystis* the electrophoretic mobility evolved slowly upon nanoparticles addition compared to *E. coli* without reaching any plateau.

As nanoparticles are positively charged in the pH range of the experiments, an electrostatic attraction naturally drives them to the cell surface. Quantification of the nanoparticles adsorption is shown on Figure 4B. It reveals a strong affinity of CeO_2

nanoparticles for *E. coli*. Indeed, small amounts of nanoparticles (up to 15 ppm) are entirely adsorbed onto the cells (Figure 4B, point C) and therefore no free CeO$_2$ is found in the solution. For larger amounts of nanoparticles, the adsorption isotherm reached a plateau meaning that these additional nanoparticles cannot bind to *E. coli* cell membranes and are detected as free CeO$_2$ within the supernatant. The beginning of the plateau of the adsorption isotherm (Figure 4B, point D) corresponds to the full charge reversal of the bacteria (Figure 4A, Point D). Considering that the specific surface area of the nanoparticles is 400 m^2/g and that their projection on a surface is 100 m^2/g, we estimate that the plateau reached for 12 mg of CeO$_2$/m^2 of cells corresponds to 1.2 m^2 of projected nanoparticles surface per m^2 of bacteria outer surface. This value confirms our previous data (Thill et al. 2006) and can be interpreted as one monolayer of nanoparticles covering the whole cells. Even if it is an estimate, these results indicate that *E. coli* can be considered as completely trapped inside a shell of CeO$_2$ nanoparticles when their concentration reaches 20–30 ppm. This conclusion applied to the present model organism obtained in highly standardized and reproducible conditions. However, exponential growth in well aerated broth or on solid agar media favors the development of afimbriate bacteria. The sensitivity of the present *E. coli* bacteria to NP toxicity may be influenced by the absence of fimbriate. Different cell membrane properties on *E. coli* could be induced using other growth conditions (like successive subculture in static broth) and may lead to different toxicity response and adsorption capacity.

The adsorption isotherm obtained for *Synechocystis* presents an unexpected shape. Indeed, for very low nanoparticles amounts, some of them remain within the supernatant. Then, for higher amounts the cells capture all nanoparticles until a plateau is reached (Figure 4A, point A). This re-adsorption of free particles at intermediate concentration is highly reproducible (much beyond the accuracy of the chemical analyse). The amplitude of the plateau (for 90 mg of CeO$_2$/m^2 cell corresponding to eight layers of CeO$_2$ nanoparticles) is highly elevated compared with *E. coli* (a single layer). These findings suggest in Synechocystis cell suspensions nanoparticles might adsorb not only onto cell membranes but also on additional materials. It is also interesting to note that in the region of the adsorption isotherm plateau, the electrophoretic mobility of the cells continues to increase even if no additional CeO$_2$ nanoparticles are adsorbed which supports the idea of a different organization of the particles around the bacteria as compared *E. coli*.

STEM images of *E. coli* and *Synechocystis* exposed to 240 ppm of CeO$_2$ nanoparticles (in the plateau region) are shown in Figure 5. The first important result of Ce-Lα XEDS elemental mapping is the absence of cerium inside both *E. coli* (Figure 5C) and *Synechocystis* cells.

E. coli presents a narrow bright line (heavy elements) closely circling its membrane (Figure 5A). An observation of the membrane at higher magnification allows the visualization of white dots corresponding to small dense individual particles covering the bacteria membranes (Figure 5B).

Ce-Lα XEDS mapping confirmed that these particles were constituted of cerium (Figure 5C). Moreover, conventional high resolution observations (Figure 5E, 5F) clearly indicated a preserved crystallinity of these CeO$_2$ particles. Thus, the direct observation of these well-individualized nanoparticles in a thin membrane layer confirmed the former adsorption and electrophoretic mobility results that nanoparticles are in very close contact with the *E. coli*'s cell membrane forming a nanoparticles shell at the adsorption isotherm plateau.

In the case of *Synechocystis* (Figure 5G) few nanoparticles are adsorbed onto the cells membranes, while large aggregates of nanoparticles are observed in the vicinity of the cells. These findings are very different to what was observed for *E. coli* the cells of which were entirely covered by nanoparticles. These data can be explained by the production of the cyanobacterial exopolymeric substances (EPS) mainly composed of polysaccharides (Panoff and Joset 1989; Duval and Ohshima 2006) which could adsorb large amounts of nanoparticles. These EPS can not be totally removed upon the washing steps prior to the exposures to nanoparticles (Figure 6).

TEM observation of EPS is difficult due to their weak binding onto cells, and to their ethanol precipitation during preparations of the samples for EPS. TEM observations (Figure 7) and XEDS cerium mapping were reproduced in absence of the ethanol dehydration procedure, where the cells fixed with glutaraldehyde were colored with alcian blue (a polysaccharides cationic stain) to compensate for the low TEM contrast of polysaccharides.

Enlarged details of both organisms revealed a major difference in the nanoparticles distributions on their cell surface. For *E. coli*, the nanoparticles were uniformly distributed onto the cell surface (black dots are nanoparticles, confirmed by XEDS cerium map not shown) and located at regular spacings from each other (Figure 7B). This may come from the existence of specific adsorption sites regularly distributed on the lipopolysaccharidic outer cell membranes (Amro et al. 2000). By contrast, the
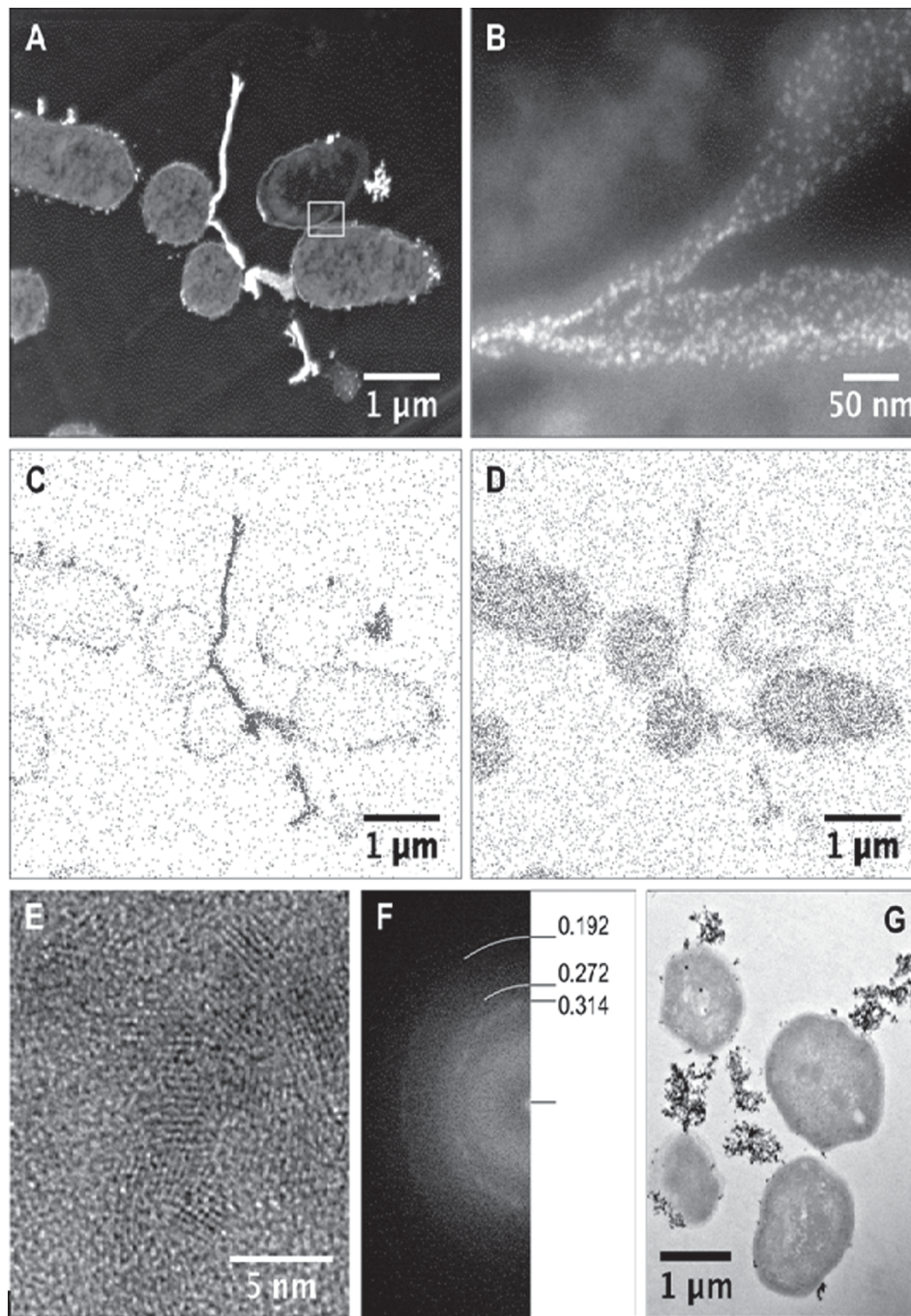
Figure 5.   TEM observations of *E. coli* and *Synechocystis* exposed to 240 ppm CeO_2 nanoparticles for 3 h in UPW. (A) STEM-HAADF image of *E. coli* cells covered with nanoparticles (bright spots). (B) enlarged detail of bacteria membranes (corresponding to the white rectangle on image A) which identifies individual CeO_2 nanoparticles (bright dots). (C) XEDS cerium map ($L\alpha$ edge) confirms the presence of cerium on *E. coli* membrane. (D) XEDS osmium map (M edge) acknowledges the presence of osmium due to sample staining. (E) HREM image demonstrating the crystallinity of CeO_2 nanoparticles, the corresponding FFT reveals interplanar spacings in agreement with the ceria structure (F). (G) TEM bright field image of several *Synechocystis* with CeO_2 nanoparticles aggregates. Scale bar: 1 μm.

distribution of nanoparticles onto *Synechocystis* is consistent with an aggregation of the nanoparticles onto the EPS at the surface. This interpretation is supported by the SEM images performed after the ethanol dehydration and removal of these EPS, which showed no remaining cerium. These findings are consistent with a previous report that CeO_2 nanoparticles aggregate in the presence of polysaccharides without forming as stable aggregates as with homopolymers (Spalla 2002).
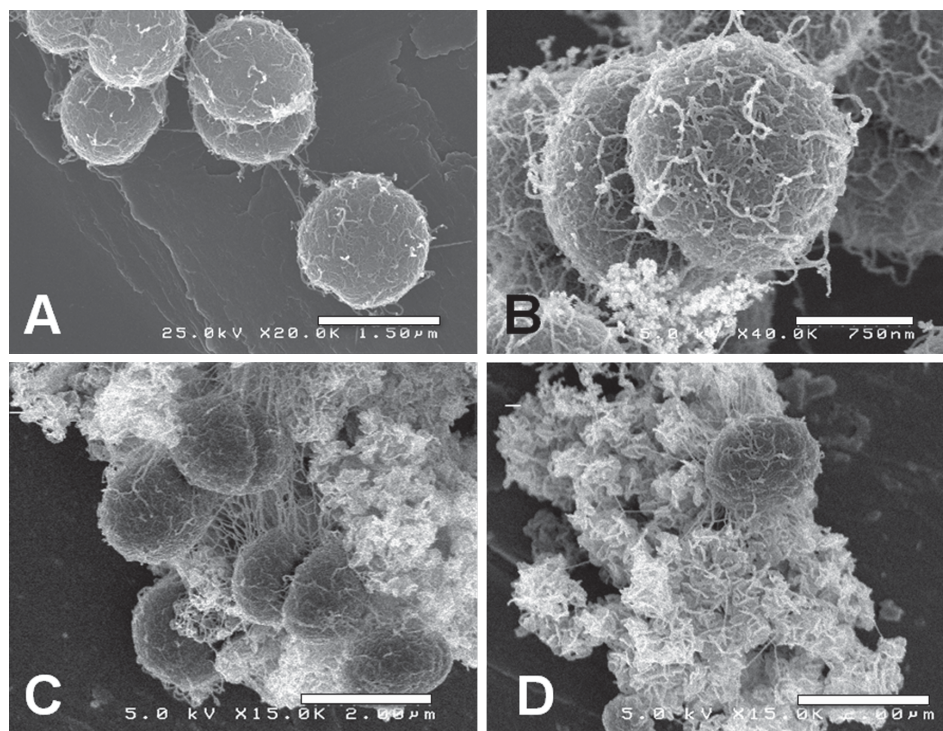
Figure 6. SEM images of *Synechocystis* fixed with 2.5% glutaraldehyde, and stained with alcian blue. (A) and (B) show views of *Synechocystis* after a classical SEM/TEM samples preparation that included several steps of dehydratation with ethanol and a CO_2 critical point drying. Pilis, but not EPS were well conserved by this procedure. (C) and (D) show *Synechocystis* dried at the CO_2 critical point in absence of ethanol dehydrating steps, a protocol that preserves EPS as well. Scale bars are respectively: A = 1.5 μm; B = 0.750 μm; C = 2 μm and D = 2 μm.

In parallel to the present microscopic study, an effective biological way to validate the influence of Synechocystis EPS on cell tolerance to NPs would be to compare the effects of NPs treatments of the wild-type strain and various *EPS depleted* mutants with a preserved good fitness. However, the construction of such EPS mutants is by no mean trivial, and out of the scope of the present study, as the many genes predicted to operate in EPS synthesis are scattered on the chromosome of *Synechocystis*.

To start investigating the role of oxido-reduction processes in the interaction between *Synechocystis*, *E. coli* and the CeO_2 nanoparticles, XANES experiments were performed on cells exposed to nanoparticles in: (i) UPW (with concentrations corresponding to the first four points of the adsorption isotherm), (ii) in their growth media (LB and MM), as well as (iii) on nanoparticles dispersed in cell-less growth media. The shapes of XANES spectra and the position of the edge are easily distinguished for Ce^{3+} and Ce^{4+} references compounds: one absorption edge at 5729 eV for Ce^{3+} and two absorption edges at 5733 eV and 5740 eV for Ce^{4+} (Figure 8).

A slight change in the redox state of CeO_2 can be easily quantified through linear combination of Ce^{3+} ($CeCl_3$) and Ce^{4+} (CeO_2 nanoparticles initial powder) reference compounds. The results of the fitting procedure are reported in Table I. The largest reduction of Ce^{4+} in Ce^{3+} is obtained in the case of *E. coli* challenged with nanoparticles in its LB growth medium (Figure 8). Indeed, a new peak clearly appears on the XANES spectra of CeO_2 nanoparticles at the energy of the Ce^{3+} even for high nanoparticles per bacteria ratio. By contrast, nanoparticles reduction driven by *Synechocystis* was in every case much weaker than that observed with *E. coli*.

The present approach monitoring the oxidation state of the nanoparticles is original as compared to the biological demonstration of oxidative stress using stress-responsive luminescent biosensors. The coupling of the two approaches is certainly a key for future studies.

Discussion

Altogether, the present results showed that *E. coli* challenged with increasing concentrations of nanoparticles is progressively covered by a thin and regular monolayer of nanoparticles surrounding the cells (Figure 7B). Finally, the rapid charge reversal, also observed for dense adsorption of nanoparticles onto
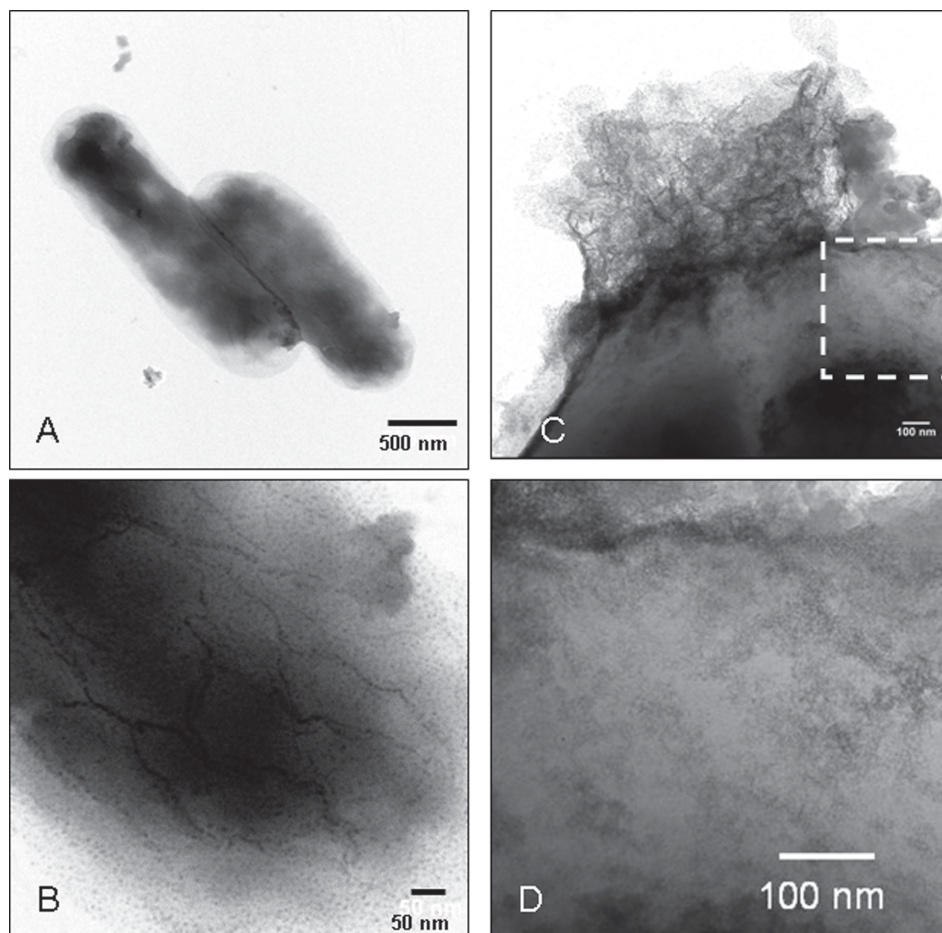
Figure 7. TEM images of *E. coli* and *Synechocystis* incubated with CeO$_2$ nanoparticles for 3 h in UPW water. The samples were fixed with glutaraldehyde and stained with alcian blue without any dehydrating steps and microtome slicing. (A) Two *E. coli* bacteria stuck together; (B) enlarged details of an *E. coli* cell surface. Blacks dots are nanoparticles uniformly covering cell membranes and pilis. (C) Part of a *Synechocystis* cell with EPS still attached to the cell. (D) Enlarged detail of the outer membrane of *Synechocystis*. Nanoparticles are not covering uniformly the outer membrane of *Synechocystis*.

well-defined solid surfaces, indicates that the outer membrane of *E. coli* offers a limited and thin surface of adsorption from an electrostatic point of view. This
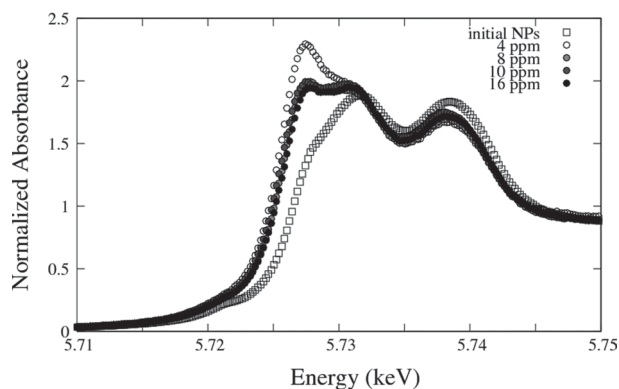
Figure 8. XANES spectra for the pellets made of *E. coli* cells exposed to increasing concentrations of CeO$_2$ nanoparticles in LB growth medium. Initial nanoparticles spectra is shown for reference.

means that the layer of adsorbed nanoparticles is relatively thin as compared to the Debye length (the characteristic length of electrostatic interaction), which is a few tens of nanometres for the ionic strength involved.

For *Synechocystis*, nanoparticles cannot form a shell at the cell surface because they are adsorbed onto the protecting layer of EPS bound to cell membranes. These nanoparticles-trapping EPS likely explains the higher level of nanoparticles adsorption onto *Synechocystis* as compared to *E. coli*. The presence of an EPS layer on *Synechocystis* also helps to understand the gradual increase in electrophoretic mobility for nanoparticles concentrations corresponding to the adsorption isotherm plateau. A thick and fuzzy layer of EPS surrounding the cells would increase their drainage and thereby decrease the electrophoretic mobility of *Synechocystis* as compared to theoretical hard particles of the same electrostatic charge. Although the full

Table I. Ce^III/Ce ratio obtained from XANES spectra at the cerium LIII edge for the nanoparticles in different media with and without bacteria.

Contact mode	Samples	Ce^III/Ce
Nanoparticles dispersed in the cell-free growth medium during 3 h	MM	<5%
	UPW	10%
	LB	10%
Bacteria incubated with nanoparticles during 3 h in UPW	*Synechocystis*	15%
	E. coli	15%
Bacteria incubated with nanoparticles during 3 h in their growth media	*Synechocystis* in MM	5%
	E. coli in LB (8, 10, 16 ppm of nanoparticles)	25%
	E. coli in LB (4 ppm of nanoparticles)	50%

description of the electrophoretic mobility of charged soft objects is a difficult task beyond the scope of this paper, theories indicate (Duval and Ohshima 2006) that the gradual increase in mobility observed upon nanoparticles adsorption is mainly due to the increase of the global electrostatic charge. In the case of *Synechocystis*, the adsorption of nanoparticles onto the EPS's layer drives the global charge of the objects from negative to positive. However, when the charge reversal begins (just at the beginning of the plateau), the layer is decorated by a fixed number of nanoparticles as shown by the isotherm of adsorption. Thereafter, the global charge of the cells cannot change. So the mobility should not change once the plateau is reached as it is observed for *E. coli* (Figure 4) for which the adsorption layer is thin. However, regarding *Synechocystis*, if we suppose that the adsorbed layer is thick and sensitive to the addition of extra nanoparticles that provide additional counter-ions increasing the ionic strength, the model of Duval and Ohshima (2006), predicts that a modification of the EPS layer thickness can induce a higher electrophoretic mobility. So the fact that the electrophoretic mobility is still increasing after the adsorption isotherm plateau may come from the compression of the EPS layer due to the screening of the interactions between the pre-adsorbed nanoparticles as ionic strength increases.

Regarding *E. coli*, the toxicity of CeO₂ nanoparticles results mainly from the direct interaction of nanoparticles with the outer cell membrane but the origin of the 'direct' toxicity remains unclear. It could be linked to the adsorption onto specific sites such as transporters and/or porins thereby interfering with nutrient transport. In that scenario,

nanoparticles-coated cells may survive for some time but would no longer divide because of starvation and would be therefore unable to generate colonies. Interestingly, we noticed that the survival of *E. coli* cells challenged with nanoparticles concentrations above the low value of 10 ppm apparently depended on the cytotoxic assays employed (CFU vs. *Live/Dead*). The *Live/Dead* observed apparent increase in survival of the *E. coli* occurred for nanoparticles amounts above what is required to reach the maximum coverage of the outer membrane (Figure 4B). This can be understood considering that the *Live/Dead*® test is based on the penetration through altered membranes of positively charged fluorescent dyes into the cells where they interact with negatively charged DNA. When positively charged nanoparticles decorate *E. coli* external membrane, they interfere with cell penetration of the positively charged *Live/Dead*® dyes thereby corrupting the reliability of this assay (but not of the CFU test that is truly based on the ability of viable cells to generate a colony). Such a phenomenon does not occur in *Synechocystis* due to the EPS that maintains the CeO₂ nanoparticles away from the cells. Indeed, the lack of correlation between the two survival tests CFU and *Live/Dead* was observed neither with *Synechocystis* challenged with nanoparticles suspensions or nanoparticles filtrate, nor with *E. coli* facing nanoparticles filtrate. As a feedback effect, it appears that the 'direct' toxicity related to the formation of a CeO₂ nanoparticles shell can also be a source of artefacts in the experiment that are designed to chase them. It is reasonable to suppose that such a perturbation of the penetration of a dye inside the cell may reveal a more general perturbation of the membrane integrity that may partly explain the survival tests.

Another potential explanation of the toxicity of CeO₂ nanoparticles in the UPW water is the generation of an oxidative stress (Thill et al. 2006). The XANES data show that only a moderate cerium reduction is observed when the CeO₂ nanoparticles are firmly adsorbed onto the outer membrane of *E. coli* in UPW thereby preventing subsequent cell division. This reduction can also be examined considering the nanometric size of the particles. Taking into account the size of the particles (7 nm) and the thickness of the surface layer (5 Å), 35–40% of the Ce atoms are localized at the surface of the nanoparticles. Assuming that the reduction of the Ce only occurred at the surface, depending on the exposure conditions, a total of 65–100% of the Ce^{4+} atoms localized at the surface have been reduced to Ce^{3+} after contact with *E. coli* whereas only 15–40% of the Ce^{4+} atoms were reduced during the contact with *Synechocystis*. Although a fraction of this reduction is

related to the dispersion of nanoparticles in abiotic media, the active role of *E. coli* in the reduction of Ce^{4+} is indisputable. This finding indicates that the 'direct' toxicity may partly be explained by an oxidative stress, either oxidation of membrane lipids or proteins compounds or capture of electrons from metabolic processes.

By contrast, the weaker toxicity of CeO_2 nanoparticles, due to pH changes, towards *Synechocystis* is consistent with the assumption that the extra-cellular cyanobacterial EPS prevent a direct contact between nanoparticles and cell membrane thereby protecting transport activities and preventing direct redox interaction at the cell surface. This pH induced toxicity is hardly possible in natural aquatic environments that contain many pH-buffering ions (carbonate, nitrate, phosphate, potassium and sodium).

Though, at first sight, the nanoparticles quantities we used seems very high as compared to what could encountered in natural environments, one needs to bear in mind that toxicity assessments require highly concentrated cell cultures, and therefore high nanoparticles doses. Furthermore, for the 'direct' toxicity the really important parameter is the ratio of the number of NPs per cell membrane surface. Natural water contains far less bacteria on average (for example 10^5 cyanobacteria per ml in ocean (Partensky et al. 1999); i.e., a value 250 times smaller than what we used). Thus, even very low concentration of CeO_2 can result in an adsorption ratio of 10 mg CeO_2 per m^2 of bacteria. Finally, from the nanoparticle side, the competition between the adsorption onto cell membranes and other adsorption target compounds needs also to be considered to know whether the toxic dose of 10 mgCeO_2 per m^2 of bacteria can be reached or not in natural conditions. We can also anticipate that CeO_2 or NPs having similar 'direct' toxic mechanism will exert a positive selection pressure for EPS-rich microbes.

Conclusion

The present analysis of the influence of CeO_2 nanoparticles on the viability of two model organisms *Synechocystis* (photoautotrophic, a representative of environmentally crucial organisms) and *E. coli* (heterotrophic, the most widely understood laboratory bacterium) demonstrates the crucial link between the physical and chemical properties of nanoparticles and their biological effects. As highlighted with *E. coli*, the direct adsorption of one monolayer of CeO_2 nanoparticles onto the cell outer membrane induces a strong toxicity. Two mechanisms are probably involved: (i) An oxidative stress triggered by the

oxidative power of Ce^{IV} atoms, and (ii) an interference of the adsorbed nanoparticles shell with the nutrient transport functions of the membrane as revealed by the fluorescent *Live/Dead* test. Both mechanisms require a direct and close contact between the nanoparticles and the bacterial membrane.

Using the model cyanobacterium *Synechocystis*, we showed the importance of the extracellular polysaccharides in the retention of nanosized CeO_2 away from the cells thereby preventing the formation of a nanoparticles shell surrounding cell membranes. This EPS mediated trapping of toxics nanoparticles away from cells is effective to prevent oxidative stress and perturbations of the membrane functions. However, it is not effective to protect the cell against 'indirect' toxicity through the release of toxic ions or molecules (Houot et al. 2007) that can diffuse through EPS.

This work highlights the crucial importance of thorough investigations of the complex physical and chemical nanoparticles/bacteria interactions to depict biological influences and toxicity of nanoparticles that are increasingly used nowadays. Toxicological studies are certainly urged by the normalization and standardization needs, but fundamental studies of nanoparticles/cell interactions as presented here must be done to define relevant protocols for *nanotoxicity* studies leading to reproducible results. For example pertinent dose metrics for 'direct' and 'indirect' nanoparticles toxicity may not be the same.

References

Amro NA, Kotra LP, Wadu-Mesthrige K, Bulychev A, Mobashery S, Liu G. 2000. High-resolution atomic force microscopy studies of the Escherichia coli outer membrane: Structural basis for permeability. Langmuir 16:2789–2796.

Auffan M, Decome L, Rose J, Orsiere T, De Meo M, Briois V, Chaneac C, Olivi L, Berge-Lefranc JL, Botta A, Wiesner MR, Bottero JY. 2006. In vitro interactions between DMSA-coated maghemite nanoparticles and human fibroblasts:

A physicochemical and cyto-genotoxical study. Environ Sci Technol 40:4367–4373.

Brayner R, Ferrari-Iliou R, Brivois N, Djediat S, Benedetti MF, Fievet F. 2006. Toxicological impact studies based on Escherichia coli bacteria in ultrafine ZnO nanoparticles colloidal medium. Nano Lett 6:866–870.

Chane-Ching JY. European Patent, EP 208580 (1987).

Chen JP, Patil S, Seal S, McGinnis JF. 2006. Rare earth nanoparticles prevent retinal degeneration induced by intracellular peroxides. Nature Nanotechnol 1:142–150.

Colvin VL. 2003. The potential environmental impact of engineered nanomaterials. Nature Biotechnol 21:1166–1170.

Derfus AM, Chan WCW, Bhatia SN. 2004. Probing the cytotoxicity of semiconductor quantum dots. Nano Lett 4:11–18.

Duval JFL, Ohshima H. 2006. Electrophoresis of diffuse soft particles. Langmuir 22:3533–3546.

Franklin NM, Rogers NJ, Apte SC, Batley GE, Gadd GE, Casey PS. 2007. Comparative toxicity of nanoparticulate ZnO, bulk ZnO, and ZnCl2 to a freshwater microalga (Pseudokirchneriella subcapitata): The importance of particle solubility. Environ Sci Technol 41:8484–8490.

Houot L, Floutier M, Marteyn B, Michaut M, Picciocchi A, Legrain P, Aude J-C, Cassier-Chauvat C, Chauvat F. 2007. Cadmium triggers an integrated reprogramming of the metabolism of Synechocystis PCC6803, under the control of the Slr1738 regulator. BMC Genomics 8:350

Kirchner C, Liedl T, Kudera S, Pellegrino T, Javier AM, Gaub HE, Stölzle S, Fertig N, Parak WJ. 2005. Cytotoxicity of colloidal CdSe and CdSe/ZnS nanoparticles. Nano Lett 5:331–338.

Ko SH, Park I, Pan H, Grigoropoulos CP, Pisano AP, Luscombe CK, Frechet JMJ. 2007. Direct nanoimprinting of metal nanoparticles for nanoscale electronics fabrication. Nano Lett 7:1869–1877.

Koksharova OA, Wolk CP. 2002. Genetic tools for cyanobacteria. Appl Microbiol Biotechnol 58:123–137.

Lu ZS, Li CM, Bao HF, Qiao Y, Toh YH, Yang X. 2008. Mechanism of antimicrobial activity of CdTe quantum dots. Langmuir 24:5445–5452.

Mai HX, Sun LD, Zhang YW, Si R, Feng W, Zhang HP, Liu HC, Yan CH. 2005. Shape-selective synthesis and oxygen storage behavior of ceria nanopolyhedra, nanorods, and nanocubes. J Phys Chem B 109:24380–24385.

Moghimi SM, Hunter AC, Murray JC. 2005. Nanomedicine: Current status and future prospects. FASEB J 19:311–330.

Minchin R. 2008. Sizing up targets with nanoparticles. Nature Nanotechnol 3:12–13.

Neal AL. 2008. What can be inferred from bacterium-nanoparticle interactions about the potential consequences of environmental exposure to nanoparticles?. Ecotoxicology 17:362–371.

Nel A, Xia T, Mädler L, Li N. 2006. Toxic potential of materials at the nanolevel. Science 311:622–627.

Oberdörster G, Stone V, Donaldson K. 2007. Toxicology of nanoparticles: A historical perspective. Nanotoxicology 1:2–25.

Ozawa M. 2006. Thermal stabilization of catalytic compositions for automobile exhaust treatment through rare earth modification of alumina nanoparticle support. J Alloys Compounds 408:1090–1095.

Panoff J, Joset F. 1989. Selection by anion-exchange chromatography of exoplysaccharide mutants of the cyanobacterium Synechocystis strain PCC-6803. Appl Environ Microbiol 55:1452–1456.

Park B, Donaldson K, Duffin R, Tran L, Kelly F, Mudway I, Morin JP, Guest R, Jenkinson P, Samaras Z, Giannouli M, Kouridis H, Martin P. 2008. Hazard and risk assessment of a nanoparticulate cerium oxide-based diesel fuel additive – a case study. Inhalat Toxicol 20:547–566.

Partensky F, Hess WR, Vaulot D. 1999. Prochlorococcus, a marine photosynthetic prokaryote of global significance. Microbiol Molec Biol Rev 63:106–127.

Pfaller T, Puntes V, Casals E, Duschl A, Oostingh GJ. 2009. In vitro investigation of immunomodulatory effects caused by engineered inorganic nanoparticles – the impact of experimental design and cell choice. Nanotoxicology 3:46–59.

Shukla R, Bansal V, Chaudhary M, Basu A, Bhonde RR, Sastry M. 2005. Biocompatibility of gold nanoparticles and their endocytotic fate inside the cellular compartment: A microscopic overview. Langmuir 21:10644–10654.

Spalla O. 2002. Nanoparticle interactions with polymers and polyelectrolytes. Curr Opin Colloid Interface Sci 7:179–185.

Spalla O, Kékicheff P. 1997. Adhesion between oxide nanoparticles: Influence of surface complexation. J Colloid Interface Sci 192:43–65.

Tarnuzzer RW, Colon J, Patil S, Seal S. 2005. Vacancy engineered ceria nanostructures for protection from radiation-induced cellular damage. Nano Lett 5:2573–2577.

Thill A, Zeyons O, Spalla O, Chauvat F, Rose J, Auffan M, Flank A. 2006. Cytotoxicity of CeO2 nanoparticles for Escherichia coli. Physico-chemical insight of the cytotoxicity mechanism. Environ Sci Technol 40:6151–6156.

Yacobi NR, Phuleria HC, Demaio L, Liang CH, Peng CA, Sioutas C, Borok Z, Kim KJ, Crandall ED. 2007. Nanoparticle effects on rat alveolar epithelial cell monolayer barrier properties. Toxicol in Vitro 21:1373–1381.

Yoon KY, Hoon Byeon J, Park JH, Hwang. 2007. Susceptibility constants of Escherichia coli and Bacillus subtilis to silver and copper nanoparticles. J Sci Total Environ 373:572–575.